Supplemental Information for

Dicer functions transcriptionally and post-transcriptionally in a multilayer antiviral defense

Ida Bagus Andika, Hideki Kondo, and Nobuhiro Suzuki‡

Institute of Plant Science and Resources, Okayama University, Kurashiki, Okayama 710-0046, Japan

‡Corresponding Author:
Nobuhiro Suzuki
Agrivirology Laboratory
Institute of Plant Science and Resources
Okayama University
Kurashiki, Okayama 710-0046, Japan
Tel. 81(86) 434-1230
Fax. 81(86) 434-1232
e-mail. nsuzuki@okayama-u.ac.jp

This PDF file includes:

- Tables S1 and S2
- Figures S1 to S13

www.pnas.org/cgi/doi/10.1073/pnas.1812407116

Supplementary tables

Table S1. List of the virus-induced gene candidates.

Transcript/protein ID	putative gene name	RPKM		DK80 vs. DK80+CHV1dp69		RPKM	DK80 vs. dsgf73+dsgf73+CHV1dp69		Annotations	ASPECT/KOG GROUP (interpro domain)
		DK80	DK80+CHV1dp69*	Fold change**	P-value	dsgf73+CHV1dp69	Fold change	P-value		
jgi|Crypa2|65641|	*gtpch*	5.332408582	1120.799266	194.9402722	0	21.02372269	3.136832771	0	GTP cyclohydrolase I	coenzyme transport and metabolism
jgi|Crypa2|287505|	*aprt*	4.161352251	451.4977753	100.7095053	0	7.70262467	1.47366059	3.0927E-05	adenine phosphoribosyl transferases	nucleotide transport and metabolism
jgi|Crypa2|327914|	*hp1*	14.42890657	1180.504224	75.91892189	0	133.0644753	7.339470286	0	hypothetical protein 1	unknown
jgi|Crypa2|231469|	*	2.714999582	209.9140978	71.70990903	0	3.466758459	1.016464982	0.90947014	D-3-phosphoglycerate dehydrogenase	amino acid transport and metabolism
jgi|Crypa2|333449|	*	3.731814731	236.1750779	58.73127293	0	21.70874288	4.630172349	0	LRR-containing protein	function unknown, protein binding (LRR_1, PNI-like)
jgi|Crypa2|349858|	*uprt*	32.81901896	1577.477377	44.62255222	0	231.0995153	5.606492658	0	uracil phosphoribosyltransferase ?	unknown (P-loop containing NTH, PRTase-like, HAD-like)
jgi|Crypa2|16211|	*btb*	2.433048838	103.3445266	39.36805506	0	8.4305625	8.4305625	0	SKP1/BTB/POZ_sf	protein binding (POZ)
jgi|Crypa2|257472|	*hel*	1.384241578	44.16869213	29.61160782	0	3.054498028	1.756555807	8.35E-08	Predicted helicase, DEAD-box superfamily	general function prediction only
jgi|Crypa2|252931|	*	3.056317516	88.45990338	26.85229	0	7.762717607	2.021432138	3.4344E-09	Cytochrome P450 subfamilies	secondary metabolites biosynthesis, transport and catabolism
jgi|Crypa2|67680|	*	4.820448367	127.8252821	24.60964099	0	22.92641285	3.78574851	0	hypothetical protein	unknown
jgi|Crypa2|44705|	*	6.321075402	116.1071998	17.04015267	0	12.40375556	1.561796097	0.00040877	GCN5-related N-acetyltransferase	metabolism
jgi|Crypa2|355436|	*	17.59281467	301.299682	15.89784129	0	7.369204131	0.333582595	0	Peptidase G1, eqolisin	proteolysis and peptidolysis
jgi|Crypa2|356052|	*hp2*	943.4194333	14518.12877	14.28688951	0	873.6288954	0.737317277	0.00012427	hypothetical protein 2	unknown
jgi|Crypa2|354844|	*	2.801971856	39.96910382	13.23442345	0	3.375650753	0.959120331	0.748103	S1/P1 nuclease	DNA catabolism
jgi|Crypa2|358414|	*	19.54377547	271.4143457	12.89089268	0	16.19007663	0.65961299	2.1849E-05	hypothetical protein	unknown
jgi|Crypa2|327709|	*	4.844512613	65.93782659	12.63175413	0	8.180847243	1.344350495	0.00508909	Cytochrome P450 subfamilies	secondary metabolites biosynthesis, transport and catabolism
jgi|Crypa2|68851|	*ac*	4.585334308	57.15889248	11.56470824	0	5.368636923	0.932128499	0.6004684	Adenylate cyclase	cAMP biosynthesis
jgi|Crypa2|266713|	*	14.59178473	174.3474755	11.08903326	0	93.62564504	5.107205576	0	GCN5-related N-acetyltransferase	metabolism
jgi|Crypa2|219629|	*	11.17087614	126.7156612	10.52832653	0	26.96888225	1.921908641	2.4649E-11	AAA+-type ATPase	posttranslational modification, protein turnover, chaperones
jgi|Crypa2|348724|	*	9.593154076	108.1374819	10.46345331	0	3.77794145	0.313652804	0	Purple acid phosphatase	carbohydrate transport and metabolism

*RPKM(Reads Per Killobases per Million)>30

Table S2. List of the primers used in this study

Name	Sequence (5`-3`)	Direction	Used for
CP-Actin (F)	GACCCAGATCGTCTTCGAGACG	Forward	RT-PCR actin
CP-Actin (R)	CGCACTTCATGATGGAGTTAAA	Reverse	RT-PCR actin
GTPcyclo(f)	CAAGGTGCTGTGCGAACTCT	Forward	RT-PCR gtph
GTPcyclo(r)	GCTCATATCAACGAGCTTGA	Reverse	RT-PCR gtph
Adeninephospho(f)	GCTACTCTCGGCACTCTAAA	Forward	RT-PCR aprt
Adeninephospho(r)	TGAAAGGAGCAAAGCAGTCC	Reverse	RT-PCR aprt
Unk327914(f)	AGCAAGGCAACGCACGCGAT	Forward	RT-PCR 27914
Unk327914(r)	AAACTTGGACTTCATCCAGC	Reverse	RT-PCR 27914
D3phospho(f)	CACAGCCACCCACGAGGTCA	Forward	RT-PCR D3
D3phospho(r)	GTGTCGTTGTGGTGATAGCG	Reverse	RT-PCR D3
LRR(f)	TCGTTCCCGACCCAAGAAAT	Forward	RT-PCR lrr
LRR(r)	GGCGGATGTGGGTGTTGGAC	Reverse	RT-PCR lrr
P-loop(f)	GGTGCTCTCGCTCAACACCT	Forward	RT-PCR uprt
P-loop(r)	CCAGCACCGTCTCCAGGTCT	Reverse	RT-PCR uprt
BTB-POZ(f)	TCGTCAAAGCACCTTACTGT	Forward	RT-PCR btb
BTB-POZ(r)	GGTGTCCAAAATTCAATGAT	Reverse	RT-PCR btb
Helicase(f)	ACGCCAAGACCTTTGGCTCA	Forward	RT-PCR helicase
Helicase(r)	TCGAGACAGTGGCAATCTCC	Reverse	RT-PCR helica
Cytochrome252931(f)	CTGGTGGCAAGATGCGTCTA	Forward	RT-PCR 252931
Cytochrome252931(r)	CGCCCTTGAGGAGGTGGCTG	Reverse	RT-PCR 252931
Threonine-serine(f)	GGATCTGCACCGAAAAGACC	Forward	RT-PCR Threo\serine
Threonine-serine(r)	TCTCGACAGCAAGCACCTTG	Reverse	RT-PCR 252931
Unk-67680(f)	GCTCCCAATCAGAATCTTGG	Forward	RT-PCR 67680
Unk-67680(r)	TAGCACCCTTTCGTGAAAGT	Reverse	RT-PCR 67680
Purple(f)	TACACCCTCTTGGATATCCT	Forward	RT-PCR Purple
Purple(r)	GGCTGGCCATGTACACTTTG	Reverse	RT-PCR Purple
Unk-356052(f)	AGTGAGAGATGCTGGCCTGG	Forward	RT-PCR 356052
Unk-356052(r)	GCATCTGAAGCGGTCTCGTT	Reverse	RT-PCR 356052
S1-P1(f)	GCTTCATACCTGCTTCTGAC	Forward	RT-PCR S1-P1
S1-P1(r)	TGCAGACGTAGGCATTTGCA	Reverse	RT-PCR S1-P1
Unk-358414(f)	ACGGCCCCTGAGATGGACCT	Forward	RT-PCR 358414
Unk-358414(r)	CAAATGTCCGCAATAGACCG	Reverse	RT-PCR 358414
CytoP450-327709(f)	AGCAAGCCGCTAGATATCGT	Forward	RT-PCR 327709
CytoP450-327709(r)	CTCGGATCATGGCCGTTCCG	Reverse	RT-PCR 327709
Adenylate(f)	CCGTCGCCATCATATCCTAT	Forward	RT-PCR ac
Adenylate(r)	GTGTAGCAGCCTCAGCCTGA	Reverse	RT-PCR ac
AAA(f)	TATCAGCTGTTACGGGCGCG	Forward	RT-PCR AAA
AAA(r)	TGCGTCCGTCGCTAGACAAA	Reverse	RT-PCR AAA
GCN5-rel(f)	GGCTCCATCACCACCCCACC	Forward	RT-PCR GCN5
GCN5-rel(r)	CAACGCCTTTACCATAATCC	Reverse	RT-PCR GCN5
Threo(f)	CGCGGCCGACAGGCACCTGC	Forward	RT-PCR 246505
Threo(r)	TGCTTCGACACCAAACTGCG	Reverse	RT-PCR 246505
LRR(f)	ACCACGGCGCCCGCCGCATC	Forward	RT-PCR lrr
LRR(r)	GTCACCAGGCTGGCGAGGGC	Reverse	RT-PCR lrr
Peptidase(f)	AAGTACGCCACTGTCGTCGC	Forward	RT-PCR Peptidase G1
Peptidase(r)	CGGACGAGGTGGTGGCCTCG	Reverse	RT-PCR Peptidase G1
Dcl2-C. parasitica(f)	CCTGCCCTGTTCAGTATCA	Forward	RT-PCR CpDcl2
Dcl2-C. parasitica(r)	GTGGTAGCCCTCTCTTTGAC	Reverse	RT-PCR CpDcl2
Dcl2-F.graminearum(f)	TCCTCAAGCGATAAGGTCATGG	Forward	RT-PCR FgDcl2
Dcl2-F.graminearum(r)	GAACTTCATCGAAGACGATAAG	Reverse	RT-PCR FgDcl2
Dcl2-R. necratix(f)	ACTACGAAAGGCTTGAATTCTT	Forward	RT-PCR RnDcl2
Dcl2-R. necratix(r)	ATCAAGGATGGGGTCACCAAGA	Reverse	RT-PCR RnDcl2
OL-327914-Neo(f)	GAATCATCAACGAATCAACCAGATACCCAGAGTTATCTCACCAT	Forward	Δ327914
OL-327914-Neo(r)	ACCCAATTCTTGCCGGCCCCTCATTCCCGGTGTAGGAAGCTGTT	Reverse	Δ327914
5arm-327914(f)	ATAACGACCGCTTCAAGGCTGT	Forward	Δ327914
5arm-327914(r)	TGAGATAACTCTGGGTATCTGGTTGATTCGTTGATGATTCGTAC	Reverse	Δ327914
3arm-327914(f)	GCTTCCTACACCGGGAATGAGGGGCCGGCAAGAATTGGGTCGGC	Forward	Δ327914
3arm-327914(r)	CACAGATTCTTAAGGCGTTGGA	Reverse	Δ327914
OL-GTP-Neo(f)	ATCTCATTCCCGCCATAACAAGATACCCAGAGTTATCTCACCAT	Forward	Δgtpch
OL-GTP-Neo(r)	TGCGATAAAGCCGCACTCTATCATTCCCGGTGTAGGAAGCTGTT	Reverse	Δgtpch
5arm-GTP(f)	ACCAGTGCAAAGGGAAAGTTTA	Forward	Δgtpch

5arm-GTP(r)	TGAGATAACTCTGGGTATCTTGTTATGGCGGGAATGAGATGAAA	Reverse	Δgtpch
3arm-GTP(f)	GCTTCCTACACCGGGAATGATAGAGTGCGGCTTTATCGCATTTG	Forward	Δgtpch
3arm-GTP(r)	GAAGCCCGGTGAGCACCTCTGG	Reverse	Δgtpch
OL-Ploop-Neo(f)	TCTCTACCGATACTGAAGCCAGATACCCAGAGTTATCTCACCAT	Forward	Δuprt
OL-Ploop-Neo(r)	TGCCATCATTCTCCTCTCTCTCATTCCCGGTGTAGGAAGCTGTT	Reverse	Δuprt
5arm-Ploop(f)	GAGAGGGAAAGGGAATGGGTTG	Forward	Δuprt
5arm-Ploop(r)	TGAGATAACTCTGGGTATCTGGCTTCAGTATCGGTAGAGAGAGT	Reverse	Δuprt
3arm-Ploop(f)	GCTTCCTACACCGGGAATGAGAGAGAGGAGAATGATGGCAAGAG	Forward	Δuprt
3arm-Ploop(r)	ACACCCCGGCTCTCCAACAAGC	Reverse	Δuprt
OL-BTB-Neo(f)	AGCCCGCAAACAGTTTCAGAAGATACCCAGAGTTATCTCACCAT	Forward	Δbtb
OL-BTB-Neo(r)	ATCTTGTTGCAGCAGCAGGTTCATTCCCGGTGTAGGAAGCTGTT	Reverse	Δbtb
5arm-BTB(f)	AAACAGAGAGTAAAAGGGATCT	Forward	Δbtb
5arm-BTB(r)	TGAGATAACTCTGGGTATCTTCTGAAACTGTTTGCGGGCTGCTG	Reverse	Δbtb
3arm-BTB(f)	GCTTCCTACACCGGGAATGAACCTGCTGCTGCAACAAGATGATA	Forward	Δbtb
3arm-BTB(r)	TAACTAGTCAGACTCATCTGCA	Reverse	Δbtb
OL-356052-Neo(f)	TCCCAATTGTCAGGGGGAACAGATACCCAGAGTTATCTCACCAT	Forward	Δ356052
OL-356052-Neo(r)	GGTAGTTTTGAGAGCTACTTTCATTCCCGGTGTAGGAAGCTGTT	Reverse	Δ356052
5arm-356052(f)	CTGTTCTTCTAAATTTCTTCGC	Forward	Δ356052
5arm-356052(r)	TGAGATAACTCTGGGTATCTGTTCCCCCTGACAATTGGGATCAT	Reverse	Δ356052
3arm-356052(f)	GCTTCCTACACCGGGAATGAAAGTAGCTCTCAAAACTACCAAAA	Forward	Δ356052
3arm-356052(r)	AGGCTGACGAGCACACGAATTT	Reverse	Δ356052
OL-Adenine-Neo(f)	CAACTTCATGCCAAGCTGACAGATACCCAGAGTTATCTCACCAT	Forward	Δaprt
OL-Adenine-Neo(r)	TTAATCATCCCCGTATCAGCTCATTCCCGGTGTAGGAAGCTGTT	Reverse	Δaprt
5arm- Adenine (f)	TGCCCCAACGACCCGGATTTTG	Forward	Δaprt
5arm- Adenine (r)	TGAGATAACTCTGGGTATCTGTCAGCTTGGCATGAAGTTGTTTT	Reverse	Δaprt
3arm- Adenine (f)	GCTTCCTACACCGGGAATGAGCTGATACGGGGATGATTAATGAA	Forward	Δaprt
3arm- Adenine (r)	GTTGGCGGCGCATAGATTGGTG	Reverse	Δaprt
OL-Adenylate-Neo(f)	GGATCCGATCATTATCAGAAAGATACCCAGAGTTATCTCACCAT	Forward	Δac
OL- Adenylate-Neo(r)	ACAAAGAAGCAGGTTTTTATTCATTCCCGGTGTAGGAAGCTGTT	Reverse	Δac
5arm-Adenylate(f)	GTACCAGCGGCGGGCCCAGGTT	Forward	Δac
5arm-Adenylate(r)	TGAGATAACTCTGGGTATCTTTCTGATAATGATCGGATCCCGTT	Reverse	Δac
3arm-Adenylate(f)	GCTTCCTACACCGGGAATGAATAAAAACCTGCTTCTTTGTACCT	Forward	Δac
3arm-Adenylate(r)	TTGGTCATGCCCACGCCGAGGA	Reverse	Δac
OL-Hel-Neo(f)	AACAACAACCACTCACTATCAGATACCCAGAGTTATCTCACCAT	Forward	Δhelicase
OL-Hel-Neo(r)	AACCAACATGGATGGGCATCTCATTCCCGGTGTAGGAAGCTGTT	Reverse	Δhelicase
5arm-Hel(f)	GTACATAGAGTCCTTGGAGATG	Forward	Δhelicase
5arm-Hel(r)	TGAGATAACTCTGGGTATCTTGACAACCAACATGGATGGGCATC	Reverse	Δhelicase
3arm-Hel(f)	GCTTCCTACACCGGGAATGAGATGCCCATCCATGTTGGTTGTCA	Forward	Δhelicase
3arm-Hel(r)	AGAAGGGCGGCGAGGCCAAGAA	Reverse	Δhelicase
HpaI-dcl2(f)	CGGCCGCAAGCTTGTTTGAGGATGGCGTACTATACCG	Forward	Pcrp:dcl2
HpaI-dcl2(r)	AGGTCAAGCATGCGTTAACCTATTTCCTCTTCAAAATCTCG	Reverse	Pcrp:dcl2
DEAH-mut(f)	GCTGCCGCAGCGCACTGCAACAAGAATCATGCCT	Forward	mutDEAD
DEAH-mut(r)	GTGCGCTGCGGCAGCGAAGACCATGAGCGCGAGTGAT	Reverse	mutDEAD
Hel2-mut(f)	GCTGCCGCAGCGGCTGCCGTGCCTGCTTGCAATCTCATCA	Forward	mutHel
Hel2-mut(r)	AGCCGCTGCGGCAGCAACGCTGGTTGCCACGAGCATA	Reverse	mutHel
RNA3a-mut(f)	GCTGCCGCAGCGGCTAGTATCCTCAAAACATGCATTA	Forward	mutRNAse-a
RNA3a-mut(r)	AGCCGCTGCGGCAGCGTCGCCTAGAAACTCAATCCTC	Reverse	mutRNAse-a
RNA3b-mut(f)	GCTGCCGCAGCGGCTGCCGCCATTCTCGACTACATCATCG	Forward	MutRNAse-b
RNA3b-mut(r)	AGCCGCTGCGGCAGCGCGGTCGTAGCACGCCACTGTT	Reverse	MutRNAse-b
DSRM-mut(f)	GCTGCCGCAGCGGCTGCCGGAAGGCTGGCGGGCAGGGAGA	Forward	mutDSRM
DSRM-mut(r)	AGCCGCTGCGGCAGCTAGCACATGCACCTGATCCCTC	Reverse	mutDSRM
HpaI-dcl2Rn(f)	CGGCCGCAAGCTTGTTGCCGAGATGTCGTCACTCATGG	Forward	Pcrp:Rn_dcl2
HpaI-dcl2Rn(r)	AGGTCAAGCATGCGTTAACTCATCCAGTCAGCATCTCATCC	Reverse	Pcrp:Rn_dcl2
HpaI-dcl2Fg(f)	CGGCCGCAAGCTTGTTATCAGGATGTCCTCAAGCGATA	Forward	Pcrp:Fg_dcl2
HpaI-dcl2Fg(r)	AGGTCAAGCATGCGTTCTAAATGAGTTCCATGGCAACA	Reverse	Pcrp:Fg_dcl2

Supplementary figures

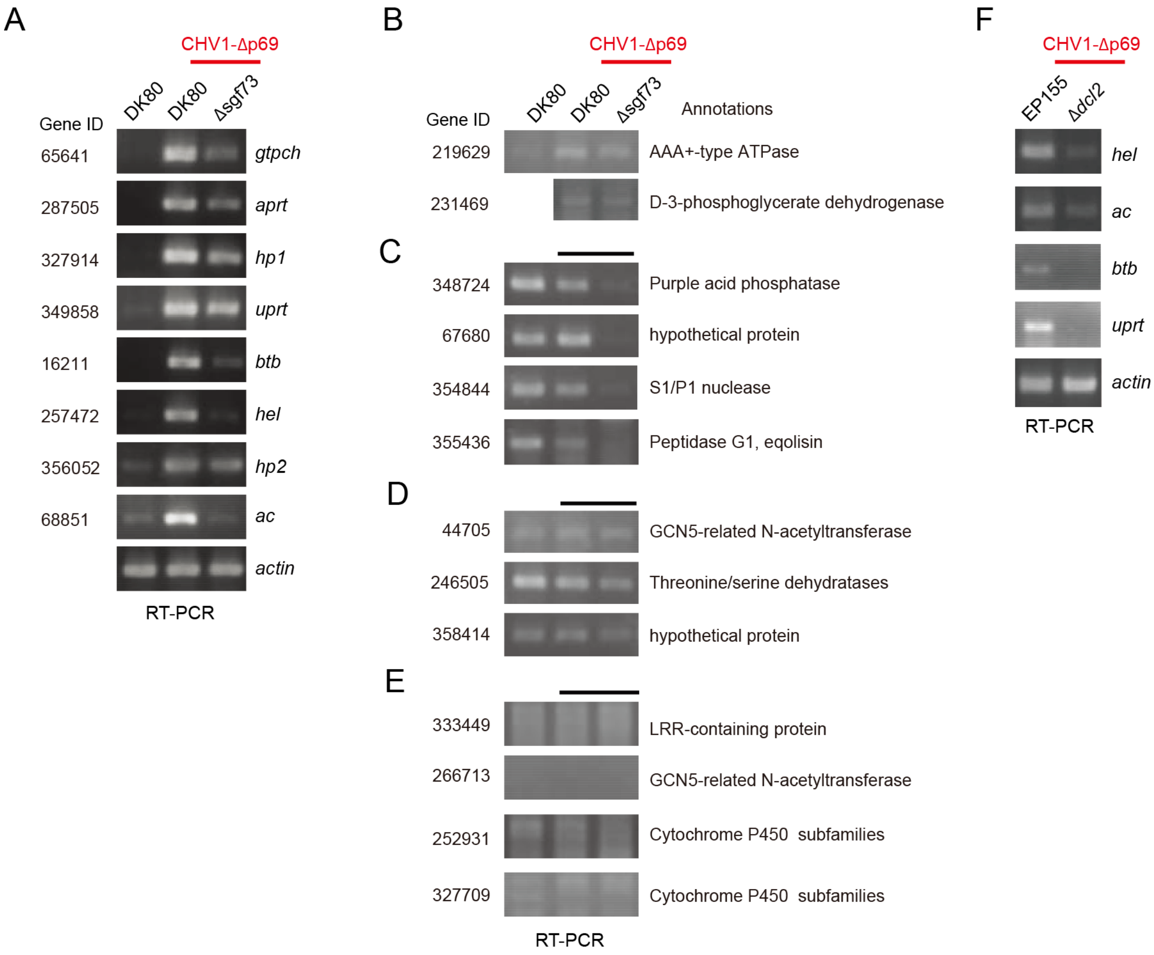

Fig. S1. RT-PCR analysis of the transcript accumulation of virus-induced gene candidates (listed in *SI Appendix*, Table S1). (A–E) Gene transcript accumulation in virus-free DK80, CHV1-Δp69-infected DK80, and Δ*sgf73* strains. The transcriptional expression pattern of genes that are highly induced by CHV1-Δp69 infection in DK80 but less induced in the Δ*sgf73* strain are shown in A, while the genes with another expression pattern or those undetected are shown in B–E. (F) Gene transcript accumulation in CHV1-Δp69-infected EP155 and Δ*dcl2* strains. The sequences of all primers used are shown in Table S2.

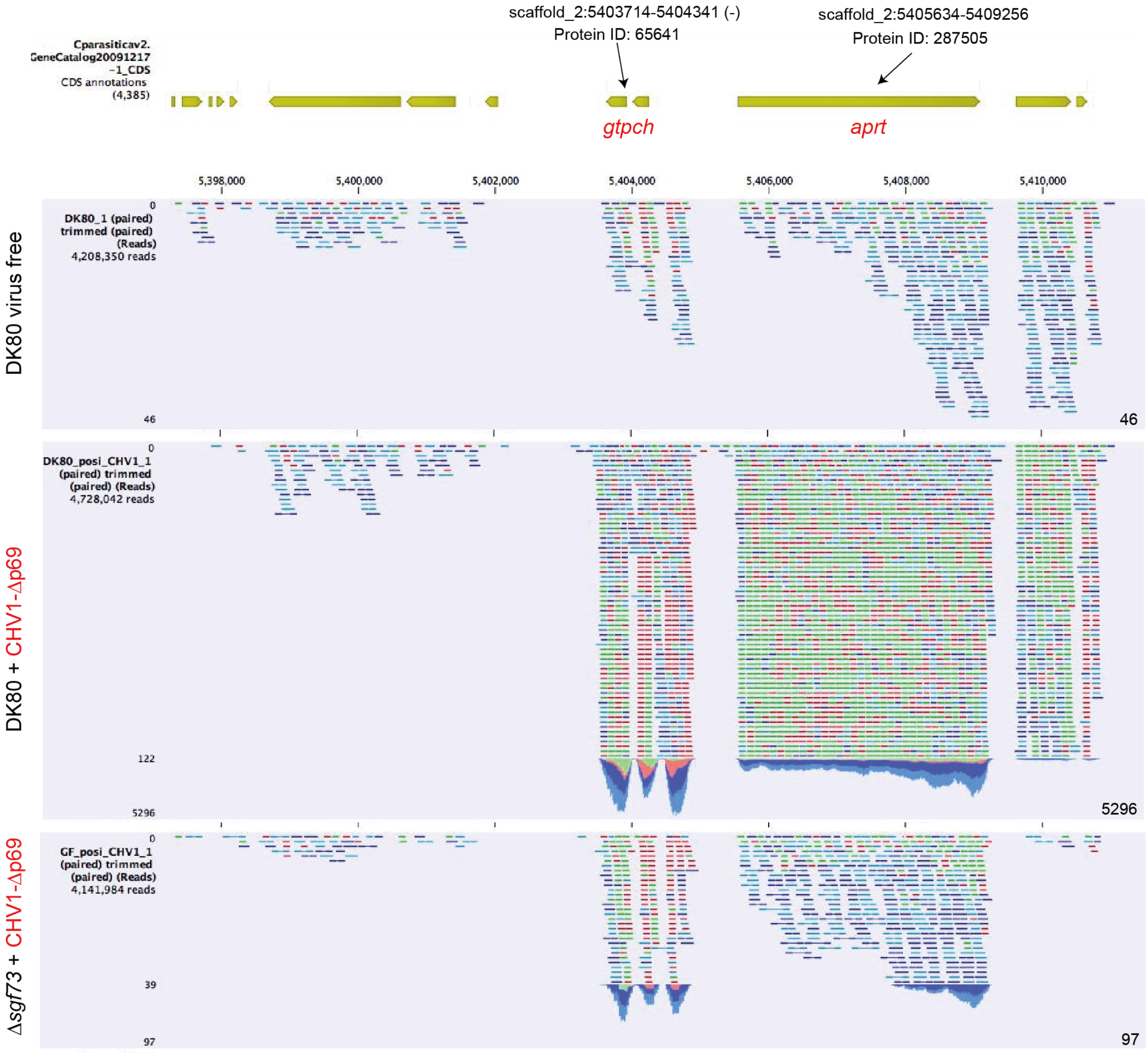

Fig. S2. Mapping positions of the *gtpch* and *aprt* genes in the *Cryphonectria parasitica* genome. Sequence reads obtained from RNA-seq analysis of virus-free DK80, CHV1-Δp69-infected DK80, and Δ*sgf73* samples are shown below the map.

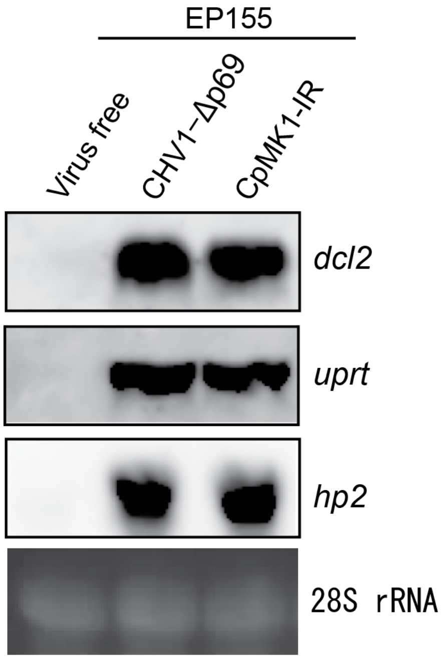

Fig. S3. Transcriptional induction of *dcl2*, *uprt*, and *hp2* by transgenic expression of inverted repeats (dsRNA). Total RNA prepared from fungal strains infected (CHV1-Δp69) or -uninfected (Virus free) by CHV1-Δp69 and expressing an inverted repeat derived from a mitogen activated kinase gene, *CpMK1* (CpMK1-IR) was subjected to Northern blotting as described in Fig. 1. Ethidium bromide-stained 28S rRNA was used as a loading control.

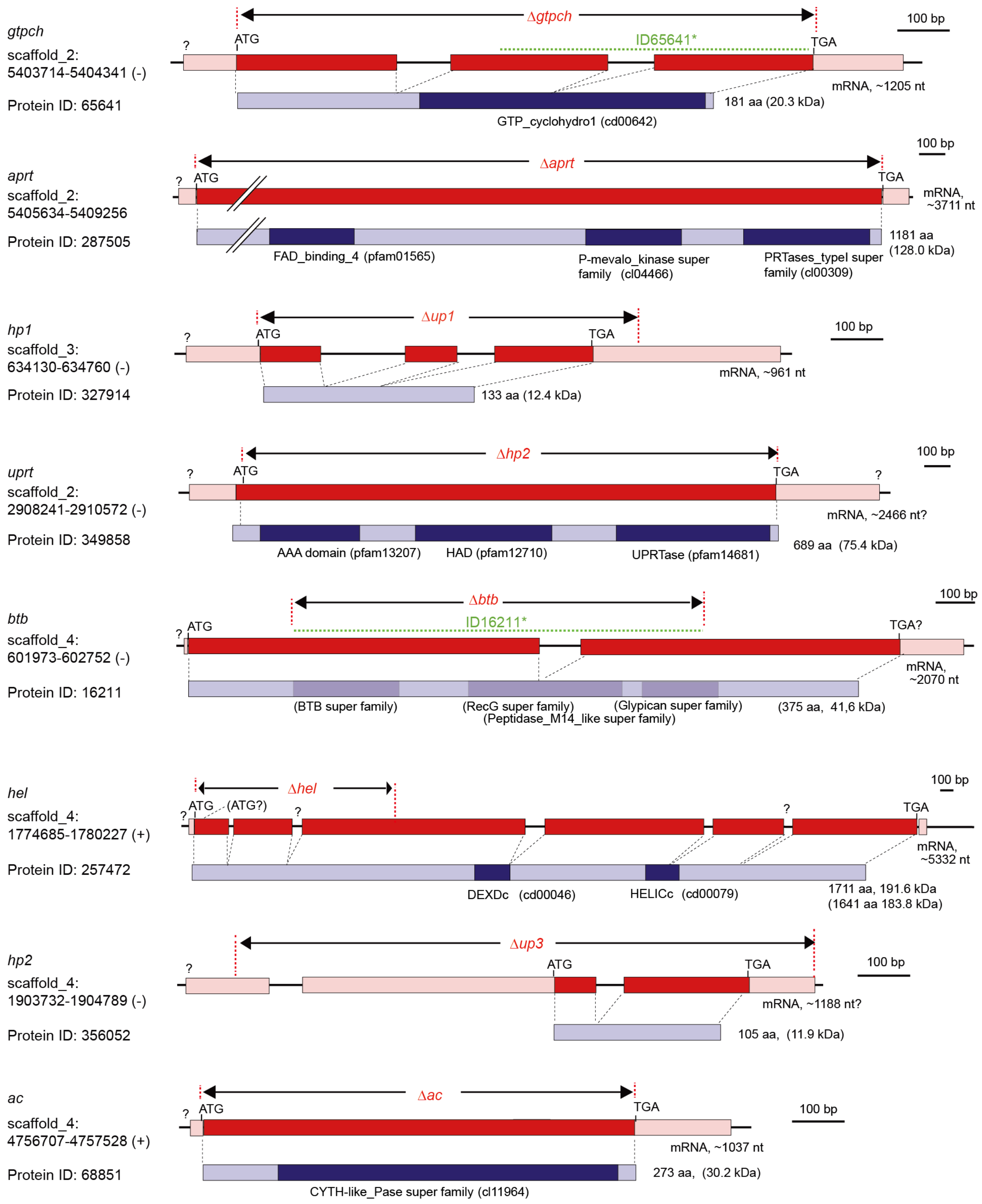

Fig. S4. Schematic representation of the selected virus-induced genes, *uprt*, *gtpch*, *aprt*, *hp1*, *hp2*, *btb*, *hel*, and *ac*. Their mapping positions in the *C. parasitica* genome (scaffold), exon/intron maps, protein ID number, protein motifs, and disrupted regions in the deletion mutants (black line with arrow head) are shown.

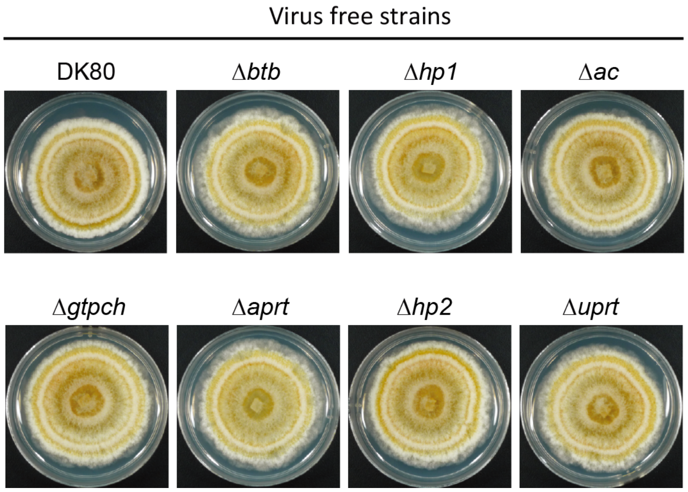

Fig. S5. Colony morphology of virus-free DK80 and the disruption mutants (Δ*uprt*, Δ*gtpch*, Δ*aprt*, Δ*hp1*, Δ*hp2*, Δ*btb*, Δ*hel*, and Δ*ac*) of *C. parasitica* on PDA plates. Fungal strains were grown on PDA for 5 days and photographed.

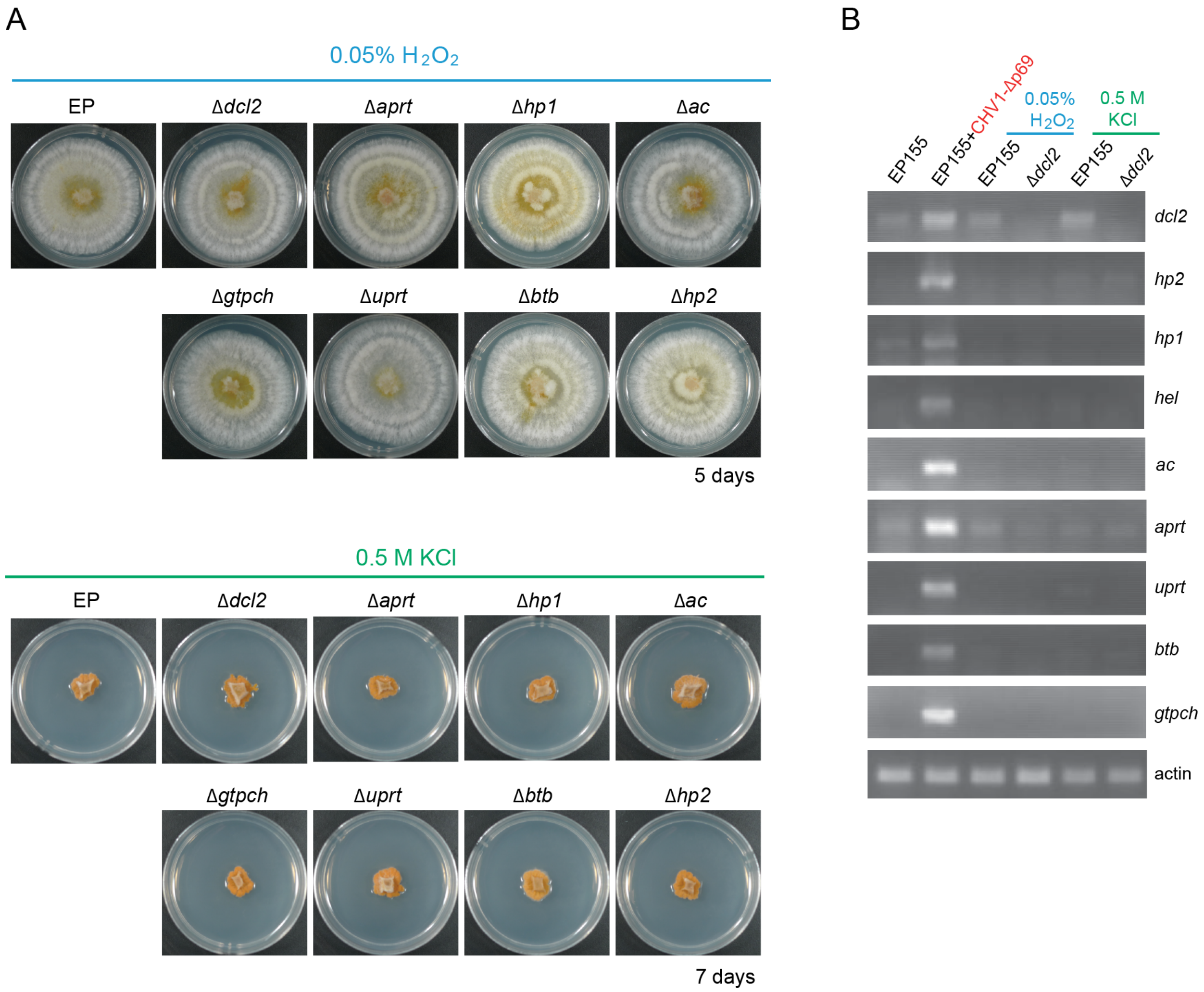

Fig. S6. Effect of oxidative and osmotic stresses on fungal growth and gene transcriptional induction. (A) Phenotype of the EP155 (EP) and DK80 disruption mutant strains (Δ*uprt*, Δ*gtpch*, Δ*aprt*, Δ*hp1*, Δ*hp2*, Δ*btb*, Δ*hel*, and Δ*ac*) on PDA medium containing 0.05% H_2O_2 or 0.5 M KCl. (B) RT-PCR analysis of gene transcriptional induction in fungal strains (EP155 and Δ*dcl2*) with or without CHV1-Δp69 infection under oxidative (0.05% H_2O_2) or osmotic (0.5 M KCl) stress. The constitutive *actin* gene was used as an internal control.

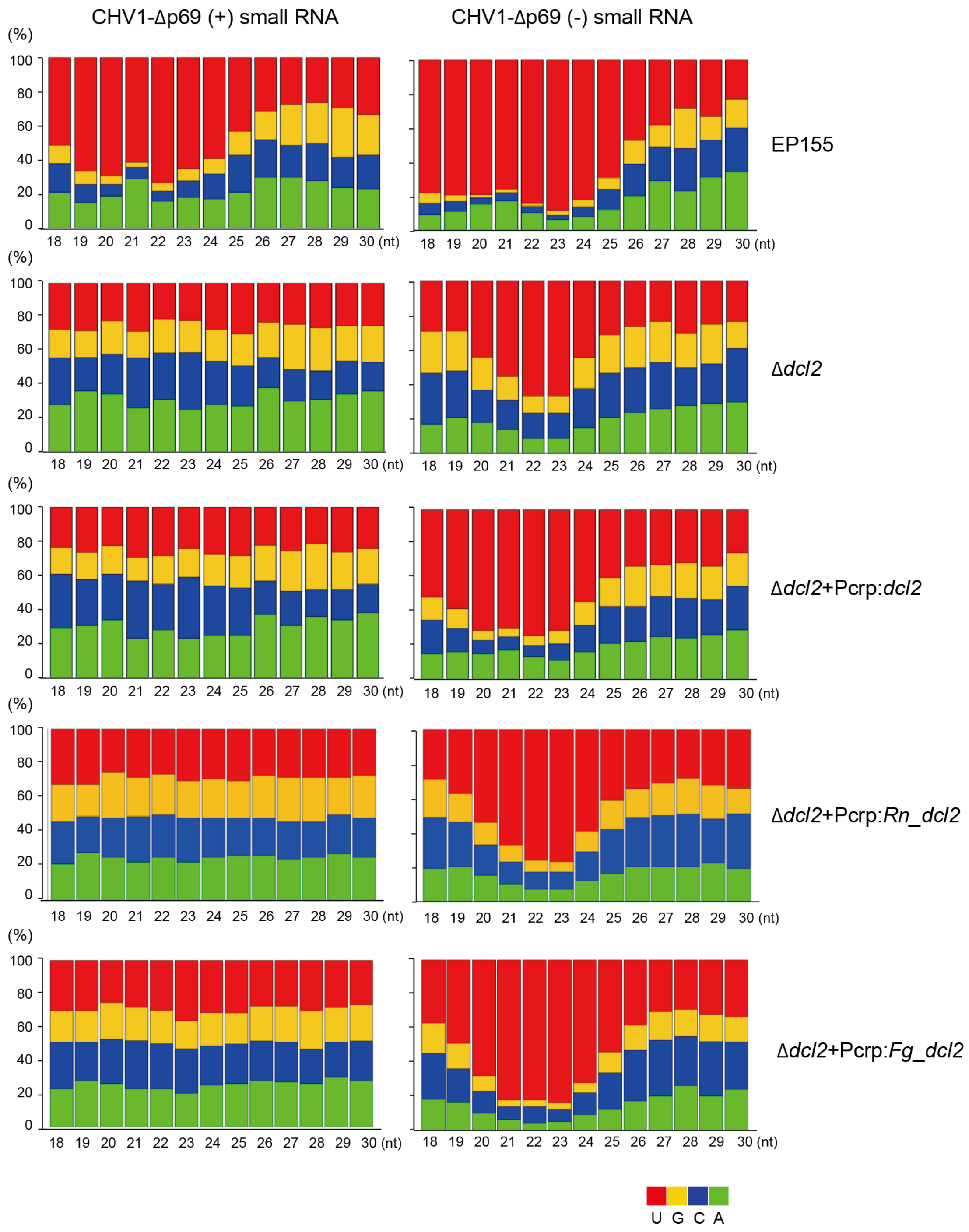

Fig. S7. 5′-terminal nucleotide profile of CHV1-Δp69-derived small RNAs from EP155, Δ*dcl2* (non-complemented), and Δ*dcl2* expressing homologous (P*crp*:*dcl2*) or heterologous DCL2 proteins from *Rosellinia necatrix* (P*crp*:*Rn_dcl2*) and *Fusarium graminearum* (P*crp*:*Fg_dcl2*). Red, dark yellow, blue and green regions denote small RNAs with 5'-terminal nucleotides U, G, C, and A, respectively.

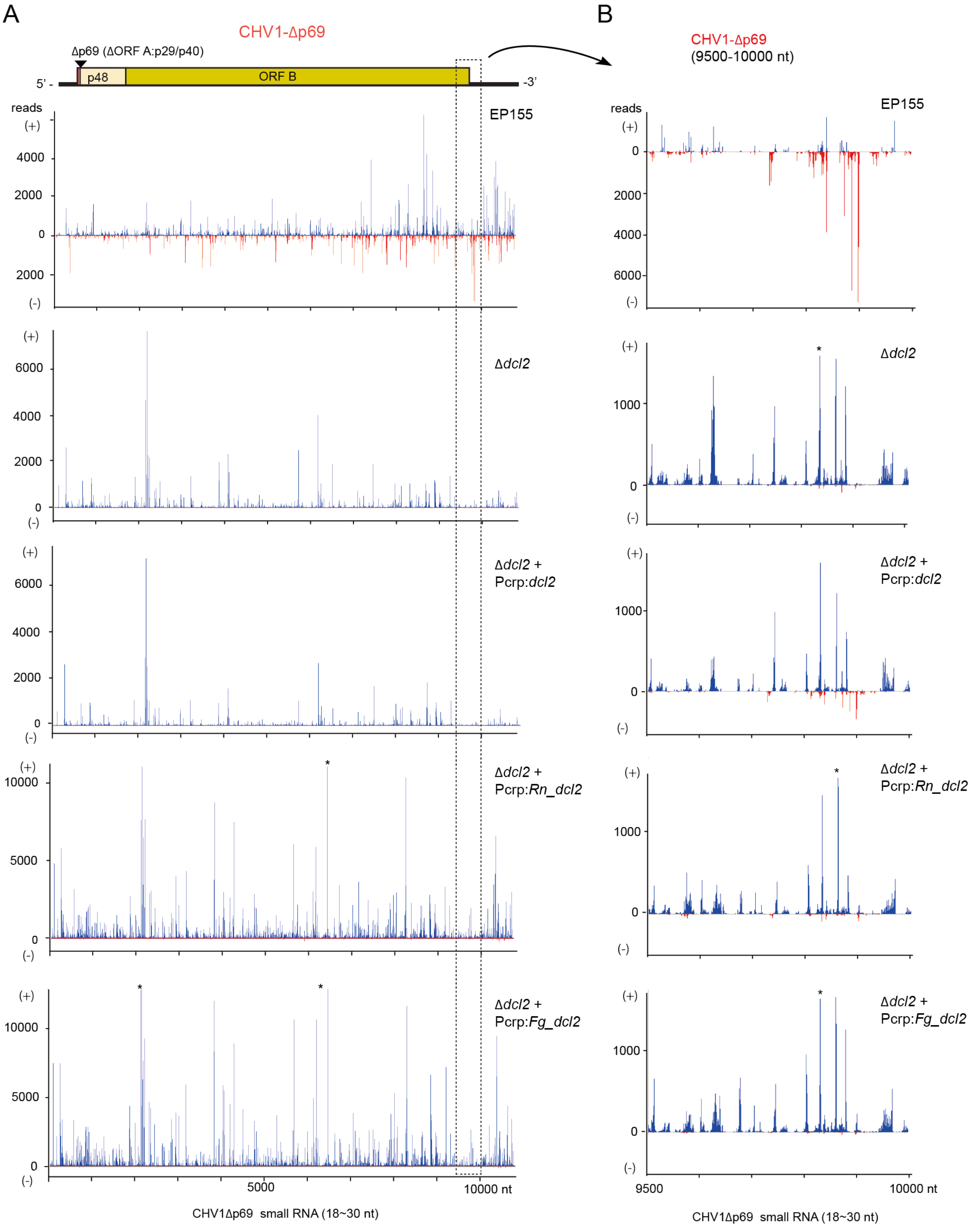

Fig. S8. Distribution of CHV1-Δp69-derived small RNAs (18–30 nt) across the viral genome. (A) Distribution map of the full-length CHV1-Δp69 genome. (B) Close-up view of small RNA distribution in a partial genome sequence (ranging 9,500–10,000 nt).

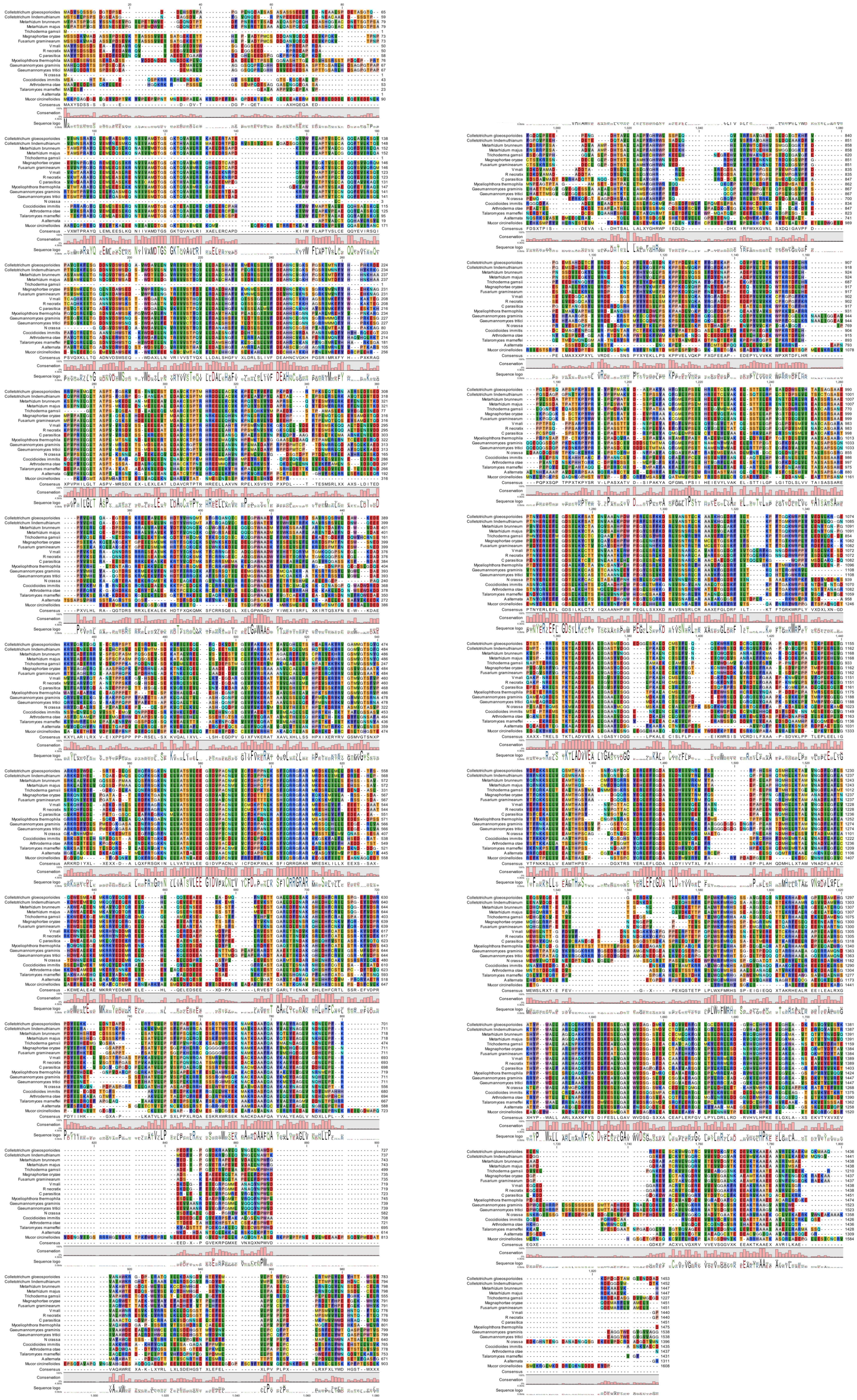

Fig. S9. Amino acid sequence alignment of DCL2 proteins from *C. parasitica* and different other selected fungi. See Fig. S11for their database accession numbers.

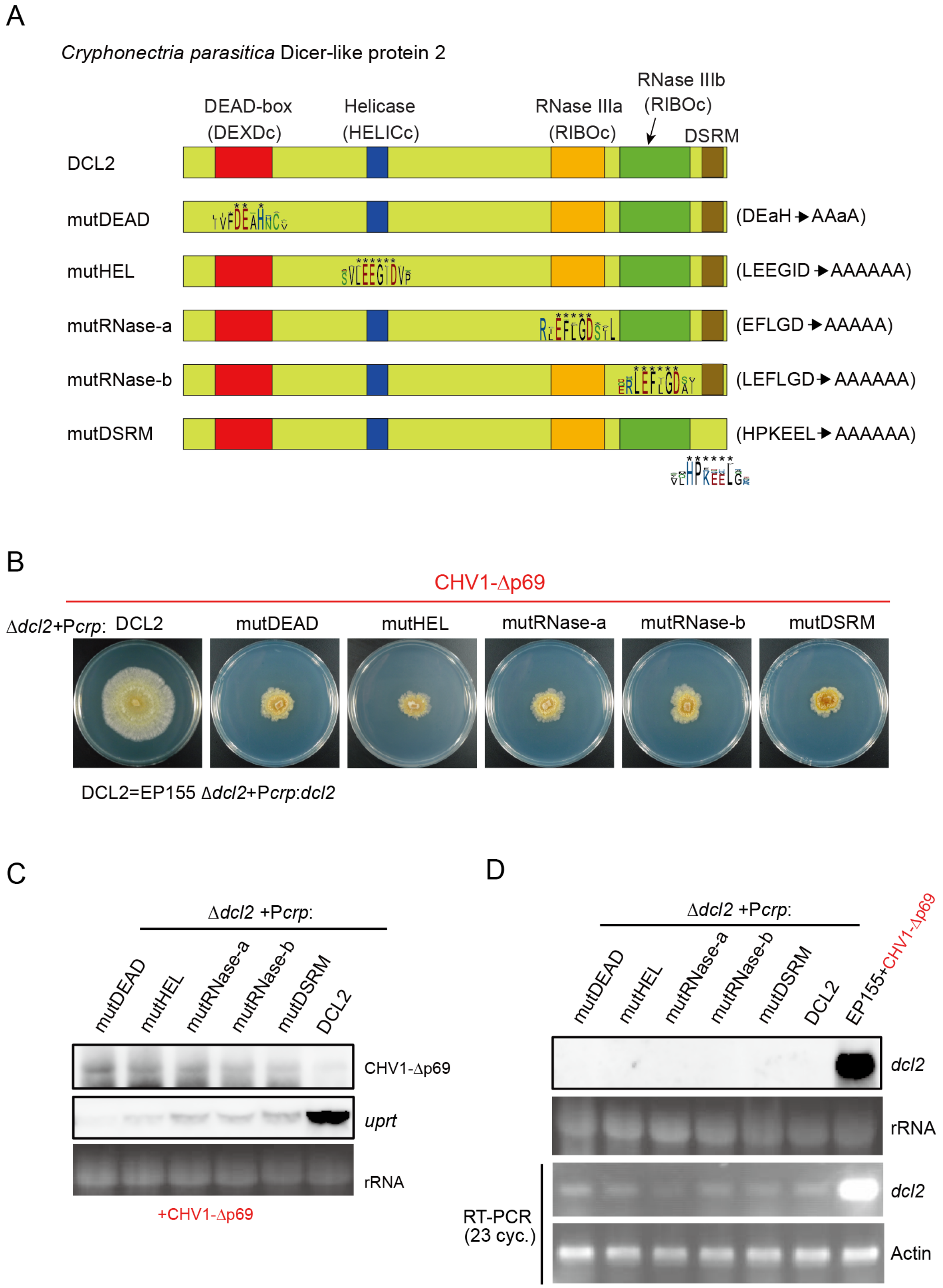

Fig. S10. Effect of mutations in protein motifs on *C. parasitica* DCL2 function. (A) Schematic diagrams showing alanine substitutions at conserved amino acid positions in helicase (DEAD-box and Helicase), ribonuclease III (RNase IIIa and IIIb, RIBOc), and dsRNA binding (DSRM) motifs in the *C. parasitica* DCL2 protein. Wild-type DCL2 is shown on the top and mutants are denoted below it. Amino acid changes in each mutant are indicated at the right. (B) Phenotype of Δ*dcl2* complemented with the *dcl2* wild-type

(DCL2) mutant constructs (mutDEAD, mutHEL, mutRNase-a, mutRNase-b and mutDSRM) described in A. The colonies were cultured for 7 days on PDA and photographed. (C) Northern blotting analysis of the CHV1-Δp69 RNA genome and *uprt* gene transcript accumulation in the fungal strains shown in B. (D) Northern blotting and RT-PCR analyses of *dcl2* transcripts in the wild-type (DCL2) and Δ*dcl2* complemented with the *dcl2* mutant constructs. Northern blotting was carried out as described in the Material and Method, while RT-PCR was performed using a primer pair, Dcl2-C. parasitica(f) and Dcl2-C. parasitica(r), Table S2).

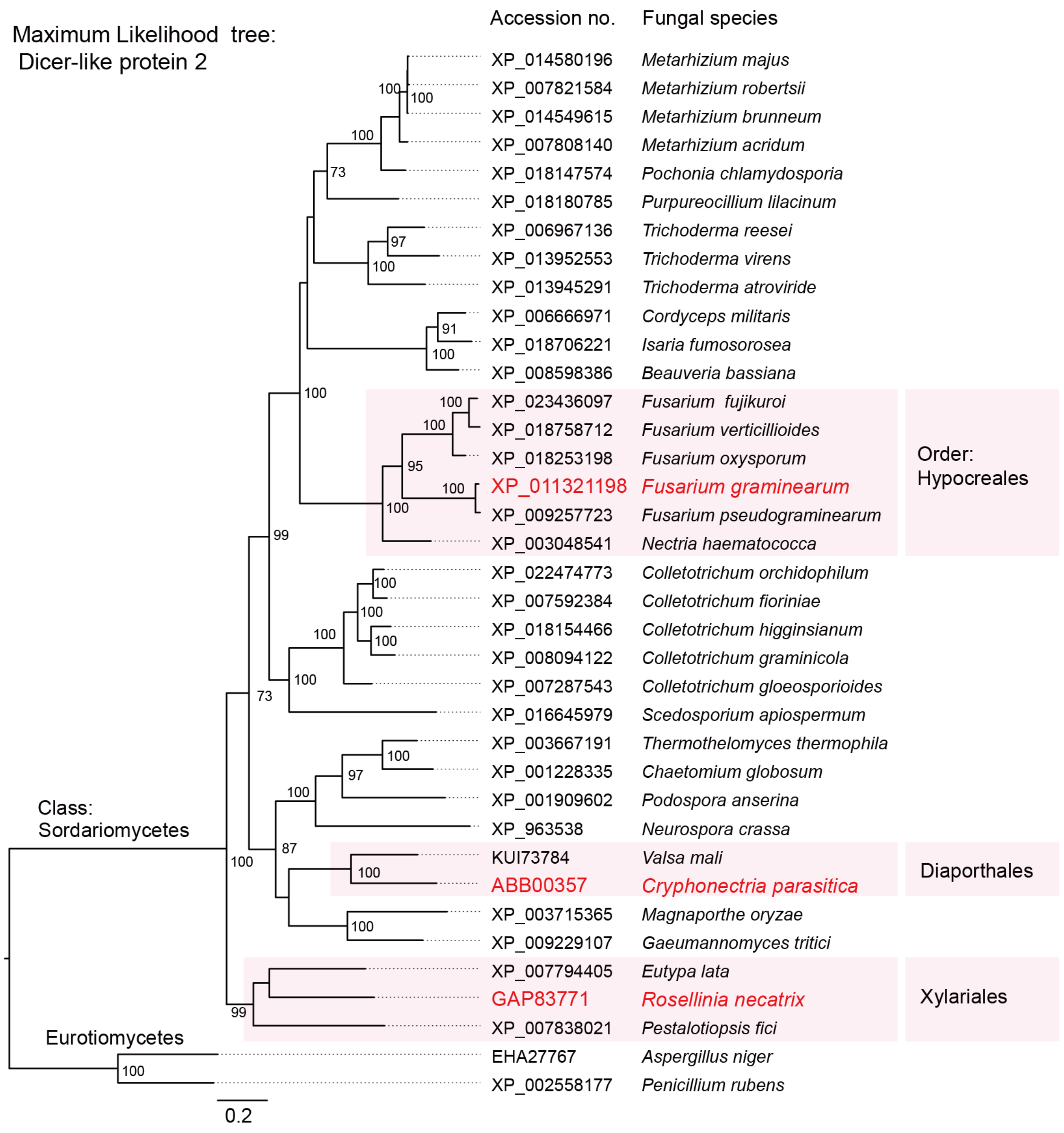

Fig. S11. Phylogenetic analysis of DCL2 proteins encoded by *C. parasitica* (order *Diaporthales*), *Rosellinia necratix* (order *Xylariales*)*, F. graminearum* (order *Hypocreales*) and different other fungi genomes. Fungal species names and database accession numbers of DCL2 proteins are indicated in the tree. The numbers at the nodes are bootstrap values of >70%.

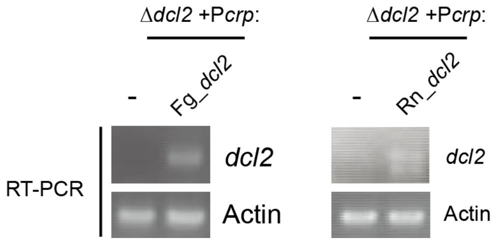

Fig. S12. RT-PCR of heterologous *dcl2* in *C. parasitica* Δ*dcl2*. Δ*dcl2* complemented with the heterologous dcl2 genes from *F. graminearum* or *R. necatrix* are described in the Fig. S7 legend. Transgenic expression of the heterologous dcl2 was confirmed by RT-PCR using primer sets, Dcl2-F. graminearum(f) and Dcl2-F.graminearum(r), and Dcl2-R. necatrix(f) and Dcl2-R. necatrix(r). See Table S2 for the primers' sequences.

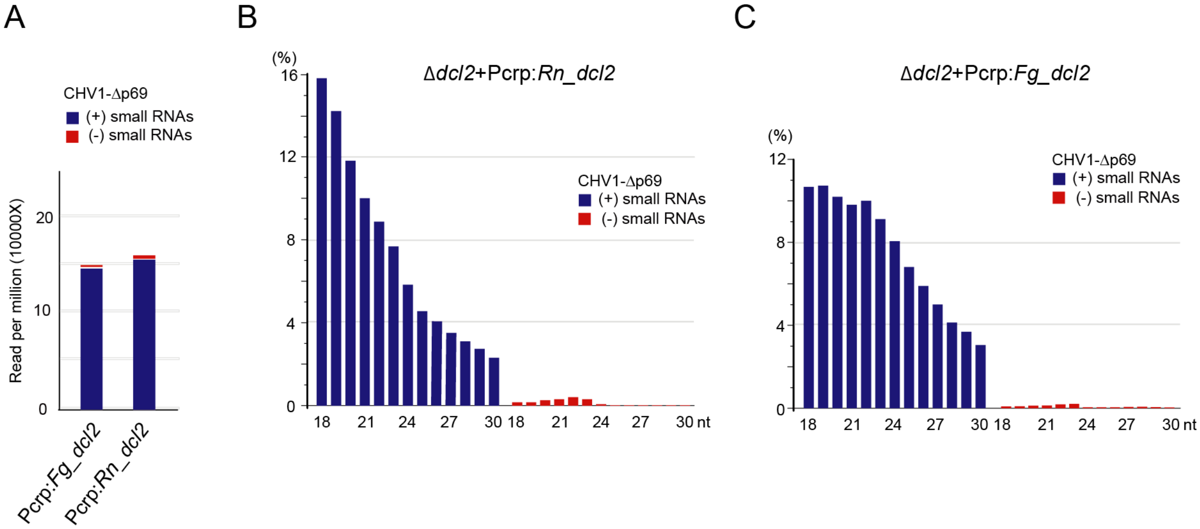

Fig. S13. Abundance (A) and size distribution (B) of CHV1-Δp69-derived small RNAs in *C. parasitica* Δ*dcl2* complemented with DCL2 from *R. necratix* (+P*crp*:*Rn_dcl2*) or *F. graminearum* (+P*crp*:*Fg_dcl2*).